ResearchGate

See discussions, stats, and author profiles for this publication at: https://www.researchgate.net/publication/255745652

Assembly and Fiber Formation of a Gemini-Type Hexathienocoronene Amphiphile for Electrical Conduction

ARTICLE *in* JOURNAL OF THE AMERICAN CHEMICAL SOCIETY · AUGUST 2013

Impact Factor: 12.11 · DOI: 10.1021/ja4062135

CITATIONS
26

READS
63

8 AUTHORS, INCLUDING:

Long Chen
Tianjin University
45 PUBLICATIONS **1,554** CITATIONS
SEE PROFILE

Kunal Mali
University of Leuven
50 PUBLICATIONS **666** CITATIONS
SEE PROFILE

Sreenivasa Reddy Puniredd
Agency for Science, Technology and Research …
48 PUBLICATIONS **762** CITATIONS
SEE PROFILE

Martin Baumgarten
Max Planck Institute for Polymer Research
279 PUBLICATIONS **4,261** CITATIONS
SEE PROFILE

Available from: Sreenivasa Reddy Puniredd
Retrieved on: 16 January 2016

JACS
JOURNAL OF THE AMERICAN CHEMICAL SOCIETY

Article

pubs.acs.org/JACS

Assembly and Fiber Formation of a Gemini-Type Hexathienocoronene Amphiphile for Electrical Conduction

Long Chen,*[,†] Kunal S. Mali,[‡] Sreenivasa R. Puniredd,[†] Martin Baumgarten,[†] Khaled Parvez,[†] Wojciech Pisula,[†] Steven De Feyter,[‡] and Klaus Müllen*[,†]

[†]Max Planck Institute for Polymer Research, Ackermannweg 10, 55128 Mainz, Rhineland-Palatinate, Germany

[‡]Division of Molecular Imaging and Photonics, Department of Chemistry, KU Leuven-University of Leuven, Celestijnenlaan, 200 F, B 3001 Leuven, Flemish Brabant, Belgium

Supporting Information

ABSTRACT: We report the synthesis, characterization, and self-assembly of a new gemini-type amphiphilic hexathienocoronene (HTC_{Gemini}), which owes its amphiphilicity to two hydrophobic dodecyl chains on one side of the HTC core and two hydrophilic triethylene glycol (TEG) chains on the other. Bearing a "softer" aromatic HTC core than the conventional hexa-*peri*-hexabenzocoronenes (HBC), and being more planar than contorted-hexabenzocoronenes (c-HBC), HTC_{Gemini} is demonstrated to yield various well-ordered assemblies in solution, at the liquid–solid interface, and in solid state by the use of different processing techniques. Regular fibers, helices, and tubes can be formed simply by processing from different solvents. At the liquid–solid interface, as visualized by scanning tunneling microscopy (STM), pairs of molecules adsorb very close to each other and arrange in the *p*2 plane group, driven by packing constraints and weak van der Waals interactions between adjacent molecules. HTC_{Gemini} also exhibits phase forming behavior in the bulk upon thermal treatment, resulting in a crystalline, herringbone-like columnar structure. Owning to an electron enriched aromatic core with respect to other reported coronenes, HTC_{Gemini} easily forms a stable radical cation, both in solution and in the bulk, upon oxidative doping with nitrosonium tetrafluoroborate ($NOBF_4$). Furthermore, light irradiation of the blend film of HTC_{Gemini} and phenyl-C_{61}-butyric acid methyl ester (PCBM) generates a prominent photocurrent which can be switched repeatedly with a large on/off ratio (6.0×10^4). The self-assembled structures obtained from HTC_{Gemini} at different length scales have potential applications in optoelectronic devices, solar cells, and redox sensors.

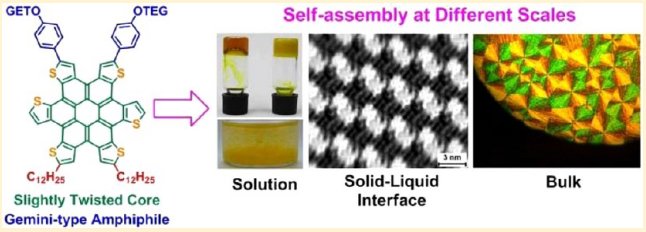

INTRODUCTION

Molecular self-assembly provides one of the most important strategies for constructing artificial nanostructures.[1] In particular, self-assembled nanostructures that consist of π-conjugated molecules have attracted increasing attention because of their potential applications in organic and supramolecular electronics.[2] Properties such as exciton diffusion or charge carrier transport largely depend on the nature of the interactions (e.g., $\pi-\pi$ stacking) among the constituent building blocks.[3,4] Other driving forces of self-assembly include hydrogen bonding,[5] electrostatic attraction,[6] host–guest recognition,[7] metal coordination,[8] charge transfer,[9] and hydrophobic–hydrophilic interactions.[10] Among them, an amphiphilic molecular design is well suited to tune the properties of organic electronic materials.[11] Amphiphilic molecules with large π-conjugated cores have been employed to obtain excellent optoelectronic properties associated with characteristic nanostructures.[10] Various amphiphiles with electronically active motifs have been observed to yield ordered aggregates in solution or bulk. Typical examples include hexa-*peri*-hexabenzocoronene (HBC),[12] naphthalene diimide,[13] perylene diimide,[14] porphyrin,[15] and fullerene[16] based amphiphiles, which tend to possess high charge carrier mobilities.

In 2004, a Gemini-shaped HBC amphiphile with two dodecyl chains and two triethylene glycol (TEG) chains on the opposite positions of the HBC core was first introduced by Aida and coworkers.[12a] These amphiphilic HBC molecules self-assembled into well-ordered nanotubes with a uniform diameter of 20 nm by helically rolling up bilayer tapes composed of stacked HBC units. Since then, various electronic functionalized nanotubes with tailored properties were developed by the same group via introducing coumarin,[12e] norbornene,[12f] trinitrofluorenone (TNF),[12g] isothiouronium ion,[12h] and pyridyl pendents[12i] at the TEG termini. Herein, we report the synthesis, characterization, and self-assembly of a highly "sulfur-doped" coronene disc (30.2 wt % of the HTC core) with a gemini-type amphiphilic molecular design inspired by Aida group's seminal work (HTC_{Gemini}, Figure 1a). HTC_{Gemini} appears to be a versatile amphiphile to form various ordered supramolecular structures through the use of different assembly conditions. Upon processing from solution, uniform fibers, helices, and tubes can be obtained by a proper choice of the solvents. The assembly processes and the morphology of the aggregates are

Received: June 20, 2013
Published: August 13, 2013

 © 2013 American Chemical Society dx.doi.org/10.1021/ja4062135 | J. Am. Chem. Soc. 2013, 135, 13531–13537

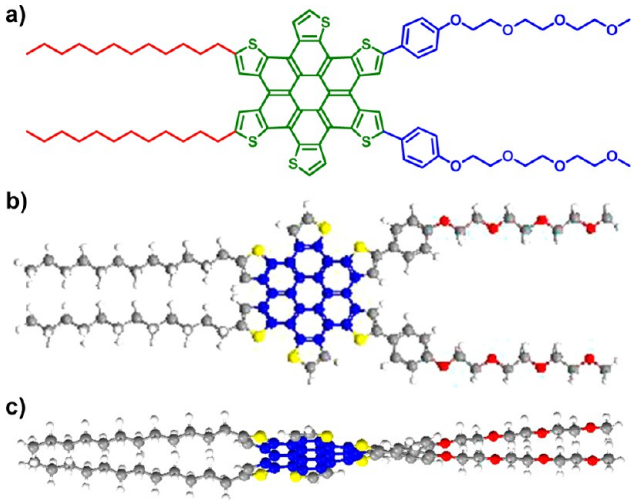

Figure 1. (a) Molecular structure; (b) top and (c) side view of simulated model[17] of HTC_{Gemini}. (C, gray or blue; S, yellow; H, white; O, red.)

characterized by UV–vis spectra and electron microscopies. When adsorbed on the surface of highly oriented pyrolytic graphite (HOPG), HTC_{Gemini} gives rise to patterns of ordered molecular pairs extending over several hundred square nanometers. In the bulk, HTC_{Gemini} is arranged in a crystalline, herringbone-like fashion in columnar structures. The derived intercolumnar lattice indicates a lamellar organization of the stacks due to dimer formation.

RESULTS AND DISCUSSION

Synthesis and Characterization. HTC_{Gemini} possesses two hydrophobic dodecyl chains on one side of the HTC core and two hydrophilic TEG chains on the other (Figure 1a). To achieve the asymmetric functionalization of the HTC core, a convergent strategy with stepwise introduction of hydrophobic and hydrophilic thiophene segments to the anthradithiophene-5,11-dione skeleton followed by photocyclodehydrogenation was adopted (Scheme 1).

The hydrophilic thiophene part **8** was synthesized from 2,4-dibromothiophene (**3**). Suzuki coupling of **3** with (4-hydroxyphenyl)boronic acid (**4**) and further nucleophilic substitution with 2-(2-(2-methoxyethoxy)ethoxy)ethyl-4-methylbenzenesulfonate (**6**) afforded compound **7**, which was converted to its pinacol boronic ester analogue **8** by Suzuki coupling with bispinacol diboron in 41% yield (3 steps). The hydrophobic part (2-dodecylthiophene-4-boronic ester) **11** was synthesized by a reported procedure.[18] On the other hand, the key building block 11-(dibromomethylene)anthra[2,3-*b*:6,7-*b*′]dithiophene-5(11H)-one (**10**) was obtained by selective Corey–Fuchs reaction of one side of the anthrabithiophene-5,10-dione (**9**) with CBr_4 and $(i\text{-PrO})_3P$. Suzuki coupling of **10** and **11** afforded intermediate **12**, which was further converted to **13** by Corey–Fuchs reaction. Next, Suzuki coupling of **13** with hydrophilic segment **8** gave the precursor **2**, which was transformed into the target compound **1** (HTC_{Gemini}) by cyclodehydrogenation. Full characterization of HTC_{Gemini} is presented in the Supporting Information (SI) (Figure S1). Electronic absorption spectra of HTC_{Gemini} in CH_2Cl_2 (SI Figure S2) display two well-resolved absorption bands at 378 and 454 nm (β, p) characteristic for large polycyclic aromatic hydrocarbons. The absorption maximum of HTC_{Gemini} (p band, 454 nm) exhibits a significant bathochromic shift (21 nm) with respect to the corresponding band of symmetric alkyl substituted HTC (433 nm),[19] which represents the extension of π-conjugation by the additional phenyl substitution on the hydrophilic side. The absorption spectra of spin-coated films disclose a bathochromic shift of 14 nm and spectral broadening, indicating a strong tendency toward aggregation (SI Figure S2).

Scheme 1. Synthesis of Asymmetric HTC_{Gemini} 1 by Stepwise Functionalization of 9

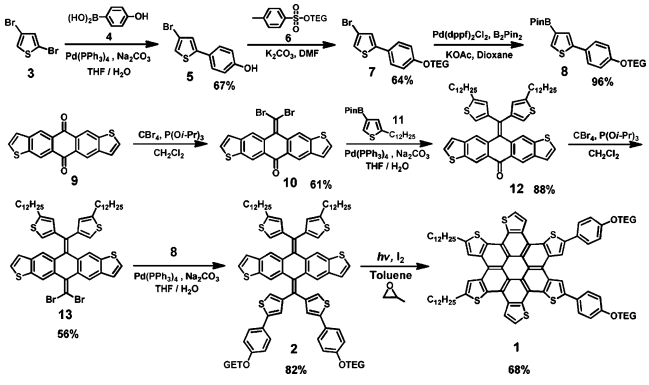

Self-assembly in Solution. The single-crystal structure of an alkyl substituted HTC analogue[19] demonstrates that the HTC core is more planar than the contorted-hexabenzocoronene (c-HBC)[20] but less planar than conventional HBC.[21] This comparison encouraged us to exploit the self-assembly of HTC_{Gemini} in various solvents. In sharp contrast to the seminal work on the gemini-shaped HBC amphiphile reported by the Aida group,[12] HTC_{Gemini} is highly soluble in THF, CH_2Cl_2, and $CHCl_3$ even at room temperature. This can be attributed to both the polyoxyethylene side-chains and the "soft" and slightly twisted HTC core as compared to the fully planar HBC core. After screening the solvents, 2-methyltetrahydrofuran (MeTHF), dioxane, and acetone were found to be better suited for the self-assembly of HTC_{Gemini} than THF, CH_2Cl_2, and $CHCl_3$. When added to MeTHF, HTC_{Gemini} was gradually dissolved upon heating up to 60 °C and produced a red-orange solution. After standing at 25 °C for several minutes, the solution formed a transparent red-orange gel A (SI Figure S3a). On heating to 70 °C, the gel of HTC_{Gemini} became a fluid and eventually turned into a solution again. The sol–gel transition was thermally reversible. The critical concentration for gelation in MeTHF was estimated to be 7 mg/mL (0.8 wt %) using the "stable to inversion of a test tube".[22] With a solvent mixture of MeTHF and MeOH (v/v = 1:1), the critical gel formation concentration could be decreased to 3 mg/mL (0.36 wt %), while forming a bright yellow opaque gel B (SI Figure S3a). Scanning electron microscopy (SEM) images of these two different gels revealed fibrous aggregates. However, the diameter of the fibers of the transparent gel A from MeTHF was significantly smaller than that of the opaque gel B formed in MeTHF/MeOH (Figure 2). High resolution SEM of gel B clearly demonstrated that the thick fibers consisted of bundles of thinner fibers (SI Figure S4).

When dioxane or acetone was added to the solid of HTC_{Gemini} at room temperature, a yellow suspension was obtained even with extensive sonication, and a completely clear solution only formed upon heating. After the hot solution was gradually cooled to room temperature, a soft cloudy precipitate was generated (SI Figure S3b). Transmission electron

dx.doi.org/10.1021/ja4062135 | J. Am. Chem. Soc. 2013, 135, 13531–13537

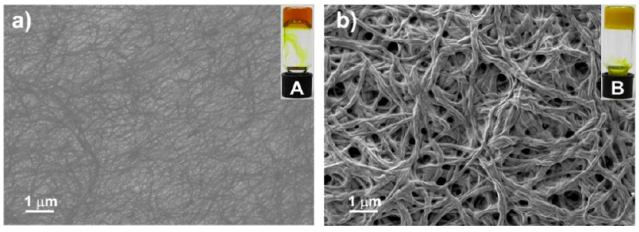

Figure 2. (a) SEM images of gel A of HTC_{Gemini} formed in MeTHF; (b) SEM images of gel B of HTC_{Gemini} formed in MeTHF/MeOH. (Inset: photograph of gels A and B.)

microscopy (TEM) images of the precipitate formed in dioxane displayed uniform helices with large aspect ratios (>1000, Figure 3a). The helices extended over several tens of

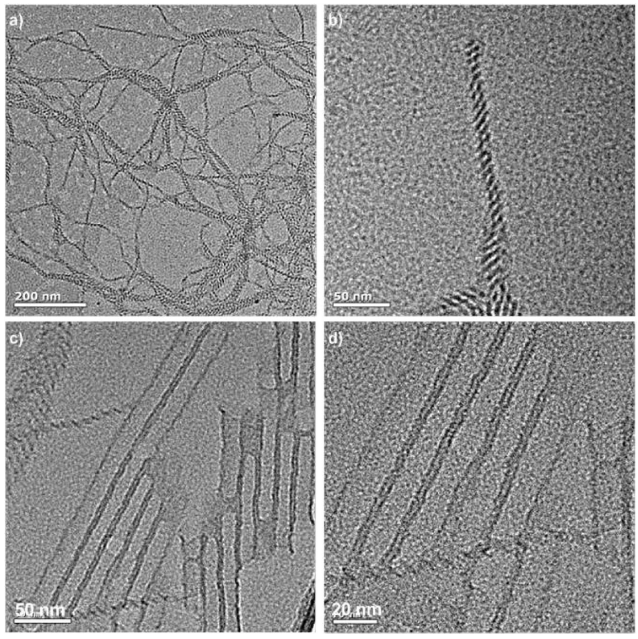

Figure 3. (a, b) TEM images of HTC_{Gemini} aggregates formed in dioxane by a heating–cooling process; (c and d) TEM images of HTC_{Gemini} aggregates formed in acetone by a heating–cooling process (scale bar = 50 nm for c; scale bar = 20 nm for part d).

micrometers while the diameter was only 12–15 nm (SI Figure S5). High resolution TEM images revealed that the pitch of such helices was around 3.4 nm (Figure 3b), corresponding to the calculated length of a bilayer of HTC_{Gemini} (3.6 nm). In contrast, the precipitates formed by a heating–cooling process in acetone mainly unveiled a completely different morphology, i.e. nanotubes with 200–300 nm in length and a uniform diameter of 20 nm (Figure 3c and d). The thickness of the wall was approximately 3.6 nm, which was related to the molecular length of the interdigitated dimer, resulting in an internal tube diameter of 13 nm.

To gain further insight into the self-assembly process, temperature dependent electronic absorption spectra were recorded at 10 °C intervals in dioxane and acetone. A bathochromic spectral shift of 7 nm was observed when cooling the hot dioxane solution of HTC_{Gemini} from 90 to 30 °C (Figure 4a). Moreover, two clear isosbestic points appeared at 435 and 458 nm, which indicated a thermoreversible assembly process. On the other hand, no obvious shift was observed in the case of acetone (Figure 4b). The aggregate formation of

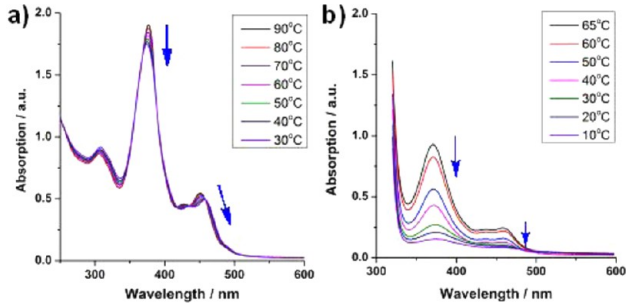

Figure 4. Temperature dependent UV–vis spectra of HTC_{Gemini} in (a) dioxane (1.7×10^{-4} M) and (b) acetone (1.0×10^{-4} M) using a 2 mm quartz cell.

HTC_{Gemini} was also examined with other binary solvent systems and monitored by UV–vis spectroscopy. For example, when adding H_2O to the THF solution (1.2×10^{-5} M) from 0 to 90%, the most intensive absorption bands at 378 and 454 nm dramatically decreased together with a bathochromic shift of 12 nm (SI Figure S7a). Other mixed solvents such as THF/MeOH, CH_2Cl_2/MeOH, dioxane/MeOH, and dioxane/H_2O gave analogous trends when increasing the polarity of the solutions (SI Figure S7b). In all cases, as observed by SEM measurements, the precipitates formed in the aforementioned binary solvents appeared to be rose-like spheres with diameters ranging from several to tens of micrometers (SI Figure S6).

To understand how the ordered fibers, helices, and tubes were formed, Fourier transform infrared spectra (FT-IR) of the isolated aggregates were measured. FT-IR spectra of the dried HTC_{Gemini} helices obtained in dioxane displayed CH_2 stretching vibrations at 2849 (ν_{sym}) and 2918 (ν_{asym}) cm^{-1} (SI Figure S8), which could be ascribed to an *all-trans* conformation, in accordance with formation of closely packed, crystalline domains.[23] Similar to other reported disc-shaped amphiphiles,[2a,11,12] HTC_{Gemini} appeared to form bilayers, driven by the van der Waals interaction of the hydrophobic alkyl chains and the π–π stacking of the HTC discs.[12−15] Their alkyl chains were well-interdigitated, thus stabilizing the bilayer structure. The repulsion between the hydrophilic TEG chains could suppress the formation of multilayer structures in polar solvents.[12] The molecular length of fully stretched HTC_{Gemini} was estimated to be 4.2 nm, while the length of the aromatic core of the interdigitated dimer was 3.6 nm, which was in good agreement with the HRTEM and XRD measurements (SI Figure S9). With all these results in mind, we proposed a molecular model to illustrate the assembly process of HTC_{Gemini} in solution, as shown in Figure 5. The molecules first form dimers by the interdigitation of dodecyl chains, which are further packed into columns *via* π–π stacking. Assisted by the interaction between hydrophilic TEG chains at the periphery of columns and the surrounding solvent molecules, these columns are eventually twisted to form helices or tubes, depending on the polarity of the solvents. In 2008, Aida group's systematic studies on the assembly of a series of different HBC molecules revealed some structural parameters being essential for the tubular assembly.[12b] It was concluded that the real essence is making the discotic π-conjugated molecule less symmetrical with two phenyl rings and sufficiently long paraffinic chains (>*n*-C_8H_{17}) on the opposite sides of the HBC unit. The hydrophilic TEG chains are not essential but helpful for growing long and robust nanotubes. Accordingly, we synthesized a symmetric bola-type amphiphile $\mathbf{1}_{TEG}$ as a model compound, where four TEG chain

dx.doi.org/10.1021/ja4062135 | J. Am. Chem. Soc. 2013, 135, 13531−13537

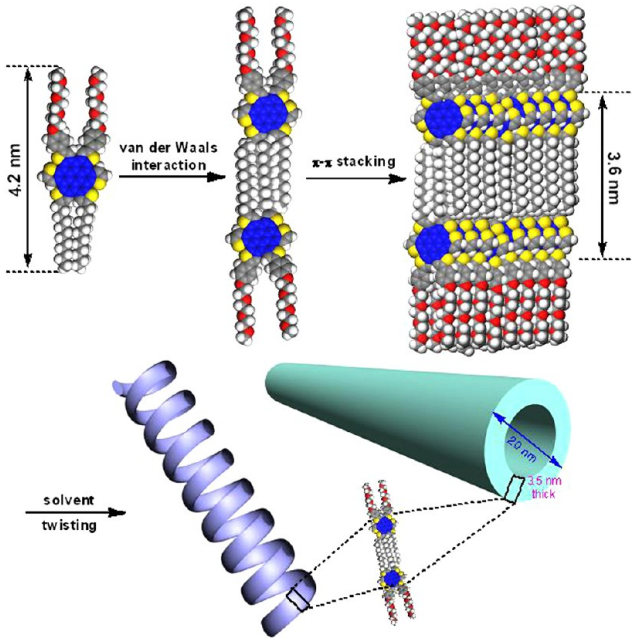

Figure 5. Schematic illustrations of the structure of self-assembled graphitic helices and nanotubes consisting of HTC_{Gemini}.

substituted phenyl rings are attached to the HTC disc. The self-assembly behavior in solution under conditions identical to those of HTC_{Gemini} was investigated (SI Figure S10). Unfortunately, ill-defined aggregates were formed in all solvent systems used for HTC_{Gemini} and neither nanofibers nor nanotubes could be observed. On the other hand, two hydrophobic HTC analogues bearing four hexyl or dodecyl chains assemble into nanorods or nanoribbons in dioxane. Thus, it can be concluded that the unsymmetric molecular design as well as the amphiphilicity of the molecule make HTC_{Gemini} a versatile platform for the generation of various ordered nanoarchitectures. Moreover, compared to the conventional rigid HBC and the heavily twisted *c*-HBC, HTCs are more flexible for processing and possess promising electronic properties which are discussed later.

Self-assembly at the Liquid–Solid Interface. In order to assess the effect of amphiphilic substituents on the lateral interactions between adsorbed molecules, the self-assembly of HTC_{Gemini} was investigated at the 1,2,4-trichlorobenzene (TCB)/highly oriented pyrolytic graphite (HOPG) interface using STM. HTC_{Gemini} forms ordered arrays of molecules that extend over several hundred square nanometers on the surface of HOPG (Figure 6a). The molecules adsorb in pairs, and two molecules in a given pair are slightly shifted with respect to each other (Figure 6b). The oblique unit cell of HTC_{Gemini} contains two molecules (plane group *p*2). The striped (orange colored) features that run approximately perpendicular to the HTC core and also parallel to one of the main symmetry axes of the HOPG lattice arise from the peripheral chains. A careful observation of the HR-STM images reveals that the striped features are not continuous on one side of each molecular core, as highlighted by the blue ovals in Figure 6b and c. The discontinuity of these features indicates partial desorption of two chains attached to the HTC core. The lack of chemical sensitivity of the STM measurements precludes unambiguous identification of the hydrophilic TEG and aliphatic chains. Nevertheless, it is readily anticipated that the striped features

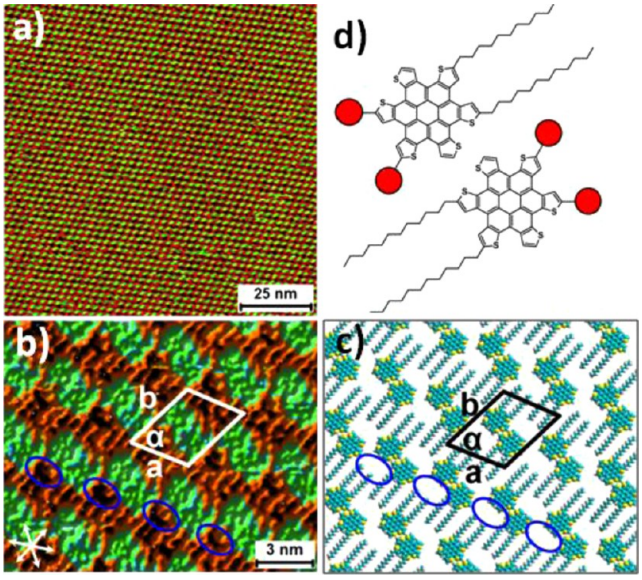

Figure 6. (a) Large area STM image of HTC_{Gemini} adsorbed at the TCB–HOPG interface. (b) High resolution STM (HR-STM) image of HTC_{Gemini} revealing partially desorbed TEG chains (blue ovals). The unit cell parameters are as follows: $a = 3.1 \pm 0.1$ nm, $b = 3.5 \pm 0.1$ nm, and $\alpha = 63.0 \pm 2.5°$. The main symmetry axes of HOPG are indicated in the lower left corner. (c) Molecular model for the packing arrangement. The TEG chains as well as the phenyl rings connecting them to the central core are omitted in the model for the sake of clarity. (d) Schematic illustration showing the relative orientation of two HTC molecules in a molecular pair.

correspond to the adsorbed dodecyl chains (SI Figure S11). This is because the interactions of the hydrophilic TEG chains with the hydrophobic HOPG surface are known to be unfavorable.[24−26] In fact, temperature programmed desorption (TPD) studies carried out on alkanes[24] and polyethylene glycol dimethyl ethers[25] (structurally similar to TEG chains) indicate that desorption barriers for alkanes are higher than those of corresponding ethers on the surface of graphite. For example, the desorption barrier (ΔE_{Des}) for $[CH_3(OCH_2CH_2)_3OCH_3]$ is 99.6 kJ/mol,[25] whereas this value is 116.9 kJ/mol[24] for dodecane, which is approximately the same chain length.[24,25] Moreover, a comparative STM investigation of amphiphilic and hydrophilic oligothiophenes also indicated that molecules with aliphatic chains tend to adsorb more strongly on the HOPG surface.[26] Thus, it is reasonable to conclude that the TEG chains are desorbed from the HOPG surface and the observed stripes in STM images arise from the aliphatic chains. The desorbed TEG chains are thus pointing toward the solution phase and are solvated by the polar TCB molecules.

The dodecyl chains are closely packed; however, there is no sign of any interdigitation. This is due to the fact that the distance between the alkyl chains on the HTC core is only 5.4 Å, which is too small for interdigitation with those of adjacent molecules.[27] Instead, the molecules adsorb on the HOPG surface in which the alkyl chains are simply adsorbed next to each other, as depicted in a molecular model shown in Figure 6c. The molecular pair formation appears to be driven by packing constraints and weak van der Waals interactions between adjacent molecules (Figure 6d). The lack of interdigitation between dodecyl chains of HTC_{Gemini} observed in the two-dimensional (2D) monolayers is in contrast to the structural information obtained from the bulk (3D) self-

dx.doi.org/10.1021/ja4062135 | J. Am. Chem. Soc. 2013, 135, 13531−13537

assembled aggregates using FT-IR and TEM, which point toward interdigitated dodecyl chains. This difference mainly arises from the presence of the substrate (HOPG) in the case of the former.

Bulk Organization. After investigating the assembly of HTC_{Gemini} in the physisorbed monolayers and the aggregates formed in solution, the ordering of its neat solid sample becomes particularly important. The bulk thermotropic properties of HTC_{Gemini} were investigated by differential scanning calorimetry and polarized optical microscopy (POM). HTC_{Gemini} exhibits one phase transition during cooling, related to solidification from the isotropic melt at 185 °C (SI Figure S12). One additional peak appears at 45 °C, which is assigned to the reorganization of the alkyl substituents. This phase was further characterized by means of cross-polarized optical microscopy of thin films cooled from the isotropic phase. Cooling HTC_{Gemini} by 5 °C/min results in a highly birefringent spherulite texture which is characteristic for crystalline phases (Figure 7a and SI Figure S13). The organization in the bulk was

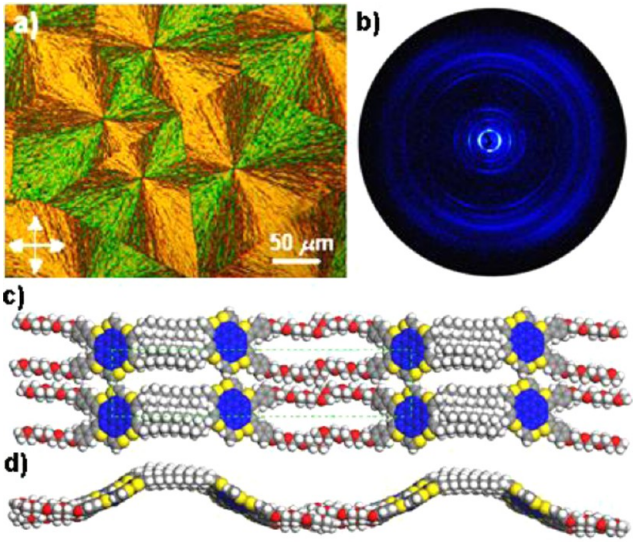

Figure 7. (a) POM image of HTC_{Gemini}; (b) 2DWAXS of HTC_{Gemini} as an extruded fiber (the fiber was mounted vertically toward the detector; meridional reflections in the small and middle angle region are due to misalignment of the columnar stacks); (c) top view and (d) side view of a rectangular 2D lattice (green dashed line: a = 71.3 Å, b = 14.5 Å; the HTC core was tilted ca. 45°) of the molecular organization model deduced from the 2D WAX analysis.

investigated by two-dimensional wide-angle X-ray scattering (2D-WAXS) on extruded fibers (1 mm in diameter). The 2D pattern discloses reflections characteristic for a crystalline phase (Figure 7b). The phase assignment is in agreement with the spherulite texture observed in POM. In this phase, the molecules form columns which are aligned along the fiber axis as indicated by distinct equatorial reflections in the small and middle angle range. Meridional scattering intensities at the same positions can be attributed to misalignment (see azimuthal integration in SI Figure S14). The unit cell for the intercolumnar organization can be described by a rectangular 2D lattice with parameters of a = 71.3 Å and b = 14.5 Å (Figure 7c, d). The lamellar-like structure with molecules organized in a herringbone arrangement leads to the appearance of only h00 reflections in the equatorial plane, whereby the 100 and 300 peaks are missing (simulation in SI Figure S15 agrees well with the experimental results). The molecular tilt toward the columnar axis is indicated by the typical off-meridional reflections, with a π-stacking distance of 3.7 Å.

Electrical Conduction of Doped Nanofibers and Photoconduction of Blended Film. To demonstrate the "bottom-up" strategy toward the construction of functional materials for electronics using the HTC system, we examined the potential electrical conduction of the ordered aggregates formed in solution upon self-assembly. To begin with, cyclic voltammetry was employed to investigate the redox processes of HTC_{Gemini}. As shown in SI Figure S16, HTC_{Gemini} in CH_2Cl_2 exhibits well-resolved consecutive oxidation steps with the first oxidation onset potentials as low as 0.19 V (vs Fc/Fc^+). The energy levels from electrochemistry are summarized in SI Table S1 for comparison. This low oxidation potential prompted us to explore the properties of radical cations.[28] Chemical oxidation of HTC_{Gemini} in CH_2Cl_2 with nitrosonium tetrafluoroborate ($NOBF_4$) afforded a new transition peak at 628 nm as well as a broad transition in the near-infrared (1035 nm), while the $\pi-\pi^*$ transition band (429 nm) of the neutral state gradually disappeared (Figure 8a). The well-organized fibers are

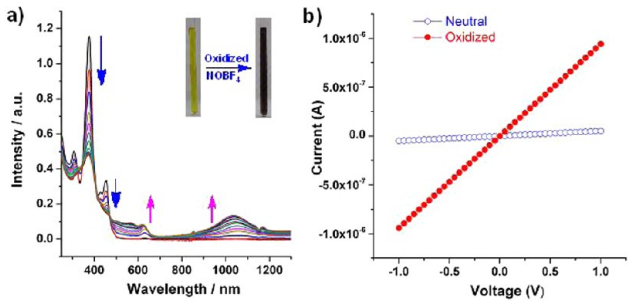

Figure 8. (a) UV titration upon adding $NOBF_4$ solution to a solution of HTC_{Gemini} in CH_2Cl_2 (1 mM); (b) $I-V$ curve of a device fabricated from the nanofibers of HTC_{Gemini} before and after oxidation with $NOBF_4$ at 25 °C.

composed of densely packed redox active building blocks which are expected to be electroconductive when charge carriers can be generated in such a highly ordered electronic array. Upon adding a solution of $NOBF_4$ in acetonitrile, a one-electron oxidant,[29] to the nanofibers of the dried gel B, the original color changed from yellow to dark brown. Electron paramagnetic resonance spectroscopy of the resulting dark brown solid displayed a resonance signal with a g value of 2.0015 (ΔH_{pp} = 0.43 mT) at 25 °C (SI Figure S17). Thus, HTC_{Gemini} can be oxidized by $NOBF_4$ to give a stable radical cation at ambient conditions. These results prompted us to further investigate the doping effect on the conductivity of these nanofibers after oxidation. SEM images show that the fibrillar structure of HTC_{Gemini} nanofibers is preserved after doping with $NOBF_4$.

We investigated this possibility by measuring the electrical conductivity across a 5 μm-wide Au gap by a two-probe method (SI Figure S18). The devices were fabricated by drop-casting an aliquot of HTC_{Gemini} gel (30 μL) onto SiO_2/Si substrates with prepatterned Au electrodes. A fixed area with bundles of fibers across the Au gap (5 μm) was selected to measure the conductivity before and also after adding $NOBF_4$. The parent nanofibers have low conductivity (blue circles), while the nanofibers after oxidation exhibit a pronounced linear $I-V$ profile with Ohmic behavior (red circles) as shown in Figure

dx.doi.org/10.1021/ja4062135 | J. Am. Chem. Soc. 2013, 135, 13531−13537

8b. The current at 1 V of the oxidized sample is amplified almost 900 times compared to the neutral species due to the formation of radical cations which facilitate the charge transport. From the $I-V$ profile of the oxidized nanofibers, the resistivity at 25 °C was calculated to be 1.1 MΩ, which is less than that for the reported amphiphilic HBC nanotubes (2.5 MΩ).[12a] The lower resistance of the doped HTC materials in comparison with that of reported doped HBC materials could be ascribed to the electron rich HTC aromatic core.[19]

Thiophene-annulated coronenes are remarkably strong electron donors and can be used as active layers in OPVs in combination with acceptors such as PCBM.[30] To assess the hole transporting properties of HTC_{Gemini}, a photodetector device[31] was fabricated by spin-coating the blend of HTC_{Gemini} and PCBM (1:2 molar ratio) onto prepatterned Au electrodes with subsequent drying in air at room temperature. The photocurrent was monitored by turning the white light illumination (20 mW/cm^2) on and off when a bias voltage of 2 V was applied. A typical on/off current switching profile is shown in Figure 9. The device exhibited a rapid response to the white light irradiation, and the generated photocurrent could be switched on−off with a large I_{on}/I_{off} ratio of 6.0 × 10^4. This value is comparable with that of the coaxial HBC-TNF nanotubes[11a] (ca. 10^4) and much higher than that of the Langmuir−Blodgett films of an anthracene supramolecular nanoribbon (ca. 40),[32] whereas it is slightly smaller when compared with that of metallosalphen dimer complex based photoconductive tapes (ca. 9.0 × 10^4).[8c]

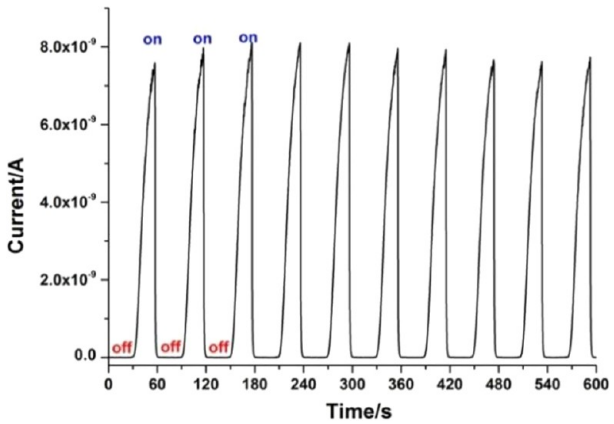

Figure 9. Photocurrent on/off switch plot when the light is turned on or off in an interval of 30 s at 2 V bias voltage.

CONCLUSION

In summary, we have synthesized a new amphiphilic disc-shaped molecule (HTC_{Gemini}) with high sulfur content in the core. Various ordered assemblies of HTC_{Gemini} can be formed in solution, at the liquid−solid interface, and in the solid state by using different processing techniques. The slightly twisted skeleton of the disc and the amphiphilicity make the molecule versatile for tuning the supramolecular structures from fibers to helices and to tubes by the choice of solution processing conditions. In the bulk, HTC_{Gemini} undergoes phase formation upon thermal treatment. The self-assembly at the liquid−solid interface leads to formation of large domains of defect-free monolayers. STM reveals a peculiar packing of molecules wherein pairs of molecules are adsorbed close to each other with their hydrophilic TEG chains pointing away from the hydrophobic HOPG surface. The strong electron donating ability of HTC_{Gemini} coupled with pronounced domain formation observed on the HOPG surface could be exploited for surface functionalization of technologically relevant substrates (e.g., graphene). The ordered nanofibers obtained from solution self-assembly of HTC_{Gemini} could be doped by $NOBF_4$, leading to the formation of stable radical cations, thus greatly enhancing the conductivity of the nanofibers. Upon irradiation with white light, the blends of HTC_{Gemini}/PCBM generate a prominent photocurrent capable of reversible switching with large on/off ratios. The self-assembled structures obtained from HTC_{Gemini} at different length scales by using different processing conditions have potential applications in optoelectronic devices, solar cells, and redox sensors.

ASSOCIATED CONTENT

Supporting Information

Synthetic details and characterization data. This material is available free of charge via the Internet at http://pubs.acs.org.

AUTHOR INFORMATION

Corresponding Authors

chen@mpip-mainz.mpg.de
muellen@mpip-mainz.mpg.de

Notes

The authors declare no competing financial interest.

ACKNOWLEDGMENTS

This work was financially supported by the DFG Priority Program SPP 1355, VW foundation (AZ. 85101-85103), and Nano-Sci-Et project SENSOR. L.C. gratefully acknowledges funding by the Alexander von Humboldt Foundation. S.R.P. acknowledges the ERC Advanced Grant NANOGRAPH (AdG-2010-267160). The authors thank Wojciech Zajaczkowski for the simulations of the X-ray data and Haixin Zhou for TEM measurement. K.S.M. acknowledges the financial assistance of (FWO), the Research Fund of KU Leuven through GOA 11/003, and the Interuniversity Attraction Poles Programme (P7/05) initiated by the Belgian Science Policy Office.

REFERENCES

(1) (a) Coleman, A. C.; Beierle, J. M.; Stuart, M. C. A.; Macia, B.; Caroli, G.; Mika, J. T.; van Dijken, D. J.; Chen, J.; Browne, W. R.; Feringa, B. L. *Nat Nano.* **2011**, *6*, 547−552. (b) Whitesides, G. M.; Grzybowski, B. *Science* **2002**, *295*, 2418−2421.

(2) (a) Hoeben, F. J. M.; Jonkheijm, P.; Meijer, E. W.; Schenning, A. P. H. J. *Chem. Rev.* **2005**, *105*, 1491−1546. (b) Wu, J.; Pisula, W.; Müllen, K. *Chem. Rev.* **2007**, *107*, 718−747.

(3) Schwartz, B. J. *Annu. Rev. Phys. Chem.* **2003**, *54*, 141−172.

(4) Sirringhaus, H.; Brown, P. J.; Friend, R. H.; Nielsen, M. M.; Bechgaard, K.; Langeveld-Voss, B. M. W.; Spiering, A. J. H.; Janssen, R. A. J.; Meijer, E. W.; Herwig, P.; de Leeuw, D. M. *Nature* **1999**, *401*, 685−688.

(5) Prins, L. J.; Reinhoudt, D. N.; Timmerman, P. *Angew. Chem., Int. Ed.* **2001**, *40*, 2382−2426.

(6) (a) Niece, K. L.; Hartgerink, J. D.; Donners, J.; Stupp, S. I. *J. Am. Chem. Soc.* **2003**, *125*, 7146−7147. (b) Zhang, X.; Wang, C. *Chem. Soc. Rev.* **2011**, *40*, 94−101.

(7) (a) Yan, X.; Wang, F.; Zheng, B.; Huang, F. *Chem. Soc. Rev.* **2012**, *41*, 6042−6065. (b) Zheng, B.; Wang, F.; Dong, S.; Huang, F. *Chem. Soc. Rev.* **2012**, *41*, 1621−1636. (c) Wang, F.; Han, C.; He, C.; Zhou, Q.; Zhang, J.; Wang, C.; Li, N.; Huang, F. *J. Am. Chem. Soc.* **2008**, *130*, 11254−11255. (d) Yu, G.; Han, C.; Zhang, Z.; Chen, J.; Yan, X.; Zheng, B.; Liu, S.; Huang, F. *J. Am. Chem. Soc.* **2012**, *134*, 8711−8717.

(e) Yu, G.; Xue, M.; Zhang, Z.; Li, J.; Han, C.; Huang, F. *J. Am. Chem. Soc.* **2012**, *134*, 13248−13251. (f) Yao, Y.; Xue, M.; Chen, J.; Zhang, M.; Huang, F. *J. Am. Chem. Soc.* **2012**, *134*, 15712−15715. (g) Yu, G.; Zhou, X.; Zhang, Z.; Han, C.; Mao, Z.; Gao, C.; Huang, F. *J. Am. Chem. Soc.* **2012**, *134*, 19489−19497. (h) Ji, X.; Yao, Y.; Li, J.; Yan, X.; Huang, F. *J. Am. Chem. Soc.* **2013**, *135*, 74−77.

(8) (a) Fujita, M. *Chem. Soc. Rev.* **1998**, *27*, 417−425. (b) Stang, P. J.; Olenyuk, B. *Acc. Chem. Res.* **1997**, *30*, 502−518. (c) Chen, L.; Wang, L.; Gao, X.; Nagase, S.; Honsho, Y.; Saeki, A.; Seki, S.; Jiang, D. *Chem. Commun.* **2009**, 3119−3121. (d) Chen, L.; Kim, J.; Ishizuka, T.; Honsho, Y.; Saeki, A.; Seki, S.; Ihee, H.; Jiang, D. *J. Am. Chem. Soc.* **2009**, *131*, 7287−7292.

(9) Wang, C.; Yin, S.; Chen, S.; Xu, H.; Wang, Z.; Zhang, X. *Angew. Chem., Int. Ed.* **2008**, *47*, 9049−9052.

(10) Shimizu, T.; Masuda, M.; Minamikawa, H. *Chem. Rev.* **2005**, *105*, 1401−1444.

(11) (a) Yamamoto, Y.; Fukushima, T.; Suna, Y.; Ishii, N.; Saeki, A.; Seki, S.; Tagawa, S.; Taniguchi, M.; Kawai, T.; Aida, T. *Science* **2006**, *314*, 1761−1764. (b) Zhang, W.; Jin, W.; Fukushima, T.; Saeki, A.; Seki, S.; Aida, T. *Science* **2011**, *334*, 340−343.

(12) (a) Hill, J. P.; Jin, W.; Kosaka, A.; Fukushima, T.; Ichihara, H.; Shimomura, T.; Ito, K.; Hashizume, T.; Ishii, N.; Aida, T. *Science* **2004**, *304*, 1481−1483. (b) Jin, W.; Yamamoto, Y.; Fukushima, T.; Ishii, N.; Kim, J.; Kato, K.; Takata, M.; Aida, T. *J. Am. Chem. Soc.* **2008**, *130*, 9434−9440. (c) Jin, W.; Fukushima, T.; Niki, M.; Kosaka, A.; Ishii, N.; Aida, T. *Proc. Natl. Acad. Sci. U.S.A.* **2005**, *102*, 10801−10806. (d) Yamamoto, Y.; Fukushima, T.; Jin, W.; Kosaka, A.; Hara, T.; Nakamura, T.; Saeki, A.; Seki, S.; Tagawa, S.; Aida, T. *Adv. Mater.* **2006**, *18*, 1297−1300. (e) Motoyanagi, J.; Fukushima, T.; Ishii, N.; Aida, T. *J. Am. Chem. Soc.* **2006**, *128*, 4220−4221. (f) Yamamoto, T.; Fukushima, T.; Yamamoto, Y.; Kosaka, A.; Jin, W.; Ishii, N.; Aida, T. *J. Am. Chem. Soc.* **2006**, *128*, 14337−14340. (g) Yamamoto, Y.; Fukushima, T.; N.; Saeki, A.; Seki, S.; Tagawa, S.; Ishii, N.; Aida, T. *J. Am. Chem. Soc.* **2007**, *129*, 9276−9277. (h) Zhang, G.; Jin, W.; Fukushima, T.; Kosaka, A.; Ishii, N.; Aida, T. *J. Am. Chem. Soc.* **2007**, *129*, 719−722. (i) Zhang, W.; Jin, W.; Fukushima, T.; Ishii, N.; Aida, T. *Angew. Chem., Int. Ed.* **2009**, *48*, 4747−4750.

(13) (a) Shao, H.; Nguyen, T.; Romano, N. C.; Modarelli, D. A.; Parquette, J. R. *J. Am. Chem. Soc.* **2009**, *131*, 16374−16376. (b) Shao, H.; Seifert, J.; Romano, N. C.; Gao, M.; Helmus, J. J.; Jaroniec, C. P.; Modarelli, D. A.; Parquette, J. R. *Angew. Chem., Int. Ed.* **2010**, *49*, 7688−7691. (c) Shao, H.; Gao, M.; Kim, S. H.; Jaroniec, C. P.; Parquette, J. R. *Chem.—Eur. J.* **2011**, *17*, 12882−12885.

(14) (a) Che, Y.; Datar, A.; Balakrishnan, K.; Zang, L. *J. Am. Chem. Soc.* **2007**, *129*, 7234−7235. (b) Zhang, X.; Chen, Z.; Würthner, F. *J. Am. Chem. Soc.* **2007**, *129*, 4886−4887. (c) Zhang, X.; Rehm, S.; Safont-Sempere, M. M.; Würthner, F. *Nat. Chem.* **2009**, *1*, 623−629.

(15) (a) Sakurai, T.; Shi, K.; Sato, H.; Tashiro, K.; Osuka, A.; Saeki, A.; Seki, S.; Tagawa, S.; Sasaki, S.; Masunaga, H.; Osaka, K.; Takata, M.; Aida, T. *J. Am. Chem. Soc.* **2008**, *130*, 13812−13813. (b) Sakurai, T.; Tashiro, K.; Honsho, Y.; Saeki, A.; Seki, S.; Osuka, A.; Muranaka, A.; Uchiyama, M.; Kim, J.; Ha, S.; Kato, K.; Takata, M.; Aida, T. *J. Am. Chem. Soc.* **2011**, *133*, 6537−6540. (c) Charvet, R.; Yamamoto, Y.; Sasaki, T.; Kim, J.; Kato, K.; Takata, M.; Saeki, A.; Seki, S.; Aida, T. *J. Am. Chem. Soc.* **2012**, *134*, 2524−2527.

(16) Muñoz, A.; Illescas, B. M.; Sánchez-Navarro, M.; Rojo, J.; Martín, N. *J. Am. Chem. Soc.* **2011**, *133*, 16758−16761.

(17) Semiempirical calculations at the AM1 level were performed with: *Spartan'04 Essential*, Version 3.0.1; Wavefunction, Inc.: Irvine, 2004.

(18) Brusso, J. L.; Hirst, O. D.; Dadvand, A.; Ganesan, S.; Cicoira, F.; Robertson, C. M.; Oakley, R. T.; Rosei, F.; Perepichka, D. F. *Chem. Mater.* **2008**, *20*, 2484−2494.

(19) Chen, L.; Puniredd, S. R.; Tan, Y.-Z.; Baumgarten, M.; Zschieschang, U.; Enkelmann, V.; Pisula, W.; Feng, X.; Klauk, H.; Müllen, K. *J. Am. Chem. Soc.* **2012**, *134*, 17869−17872.

(20) Xiao, S.; Myers, M.; Miao, Q.; Sanaur, S.; Pang, K.; Steigerwald, M. L.; Nuckolls, C. *Angew. Chem., Int. Ed.* **2005**, *44*, 7390−7394.

(21) Pisula, W.; Kastler, M.; Wasserfallen, D.; Pakula, T.; Müllen, K. *J. Am. Chem. Soc.* **2004**, *126*, 8074−8075.

(22) Sobczuk, A. A.; Tamaru, S.-i.; Shinkai, S. *Chem. Commun.* **2011**, *47*, 3093−3095.

(23) (a) Chen, Y.; Zhu, B.; Zhang, F.; Han, Y.; Bo, Z. *Angew. Chem., Int. Ed.* **2008**, *47*, 6015−6018. (b) Masuda, M.; Shimizu, T. *Langmuir* **2004**, *20*, 5969−5977.

(24) Paserba, K. R.; Gellman, A. J. *Phys. Rev. Lett.* **2001**, *86*, 4338−4341.

(25) Paserba, K. R.; Vaidyanathan, N.; Gellman, A. J. *Langmuir* **2002**, *18*, 9799−9809.

(26) Surin, M.; Leclere, P.; De Feyter, S.; Abdel-Mottaleb, M. M. S.; De Schryver, F. C.; Henze, O.; Feast, W. J.; Lazzaroni, R. *J. Phys. Chem. B* **2006**, *110*, 7898−7908.

(27) Tahara, K.; Johnson, C. A., II; Fujita, T.; Sonoda, M.; De Schryver, F. C.; De Feyter, S.; Haley, M. M.; Tobe, Y. *Langmuir* **2007**, *23*, 10190−10197.

(28) Nielsen, C. B.; Angerhofer, A.; Abboud, K. A.; Reynolds, J. R. *J. Am. Chem. Soc.* **2008**, *130*, 9734−9746.

(29) Arikainen, E. O.; Boden, N.; Bushby, R. J.; Clements, J.; Movaghar, B.; Wood, A. *J. Mater. Chem.* **1995**, *5*, 2161−2165.

(30) (a) Gorodetsky, A. A.; Chiu, C.-Y.; Schiros, T.; Palma, M.; Cox, M.; Jia, Z.; Sattler, W.; Kymissis, I.; Steigerwald, M.; Nuckolls, C. *Angew. Chem., Int. Ed.* **2010**, *49*, 7909−7912. (b) Kang, S. J.; Kim, J. B.; Chiu, C.-Y.; Ahn, S.; Schiros, T.; Lee, S. S.; Yager, K. G.; Toney, M. F.; Loo, Y.-L.; Nuckolls, C. *Angew. Chem., Int. Ed.* **2012**, *51*, 8594−8597.

(31) Pang, S.; Yang, S.; Feng, X.; Müllen, K. *Adv. Mater.* **2012**, *24*, 1566−1570.

(32) Zhang, Y.; Chen, P.; Jiang, L.; Hu, W.; Liu, M. *J. Am. Chem. Soc.* **2009**, *131*, 2756−2757.